Two-Electron Escape Near Threshold: A Classical Process?

Jan-Michael Rost

Harvard University, Lyman Laboratories of Physics, Cambridge, Massachusetts 02138 (Received 10 September 1993)

For electron impact ionization of hydrogen the S matrix is determined by calculating Feynman's path integral semiclassically. The total ionization probability is in excellent agreement with the experiment. At a critical excess energy of $3.3~{\rm eV}$ the differential cross section for the energy sharing between the continuum electrons undergoes a qualitative change which limits the range of the threshold behavior. The Wannier threshold law is confirmed, but only in the limit of vanishing excess energy.

PACS numbers: 34.80.Dp, 03.65.Sq, 31.10.+z

Forty years ago, Wannier derived what is today known as the "Wannier law" for double electron escape in an atom at threshold. By using classical mechanics, he showed that the total cross section as a function of excess energy follows a power law, different from the linear behavior for single electron escape [1]. Since then the phenomenon has been under intensive investigation, experimentally [2, 3] as well as theoretically [4–8]. A new generation of experiments [9, 10] gave hints for "structure" in the measurable quantities which is excluded by the original Wannier law as well as by the quantum mechanical WKB predictions. The experimental findings have drawn attention to an alternative explanation of the threshold behavior by Temkin who predicted a linear threshold law modulated by oscillations [6]. All major theoretical approaches suffer from the impossibility of providing a full scattering amplitude, since they are either classical (Wannier) or based on modeling an approximate wave function for two-electron escape in a limited part of the configuration space only.

Here, we will describe the two-electron escape within the S-matrix formalism. In this way, the scattering amplitude is well defined. In a true scattering formulation, the two-electron escape depends on its "past," i.e., the way the escape was initiated. We choose ionization from the ground state of hydrogen. The explicit consideration of an initial state also provides an absolute energy scale for the escape cross section and allows direct comparison with the experiment [2, 10].

We do not attempt to calculate the propagator of the S matrix exactly, which is at least for the time being impossible for energies close to threshold [11]. Rather, we evaluate the S matrix, i.e., Feynman's path integral, semiclassically. Only the properties of classical trajectories are needed when the quantum propagator $\exp[-iHt/\hbar]$ is replaced by its semiclassical limit, as given by van Vleck [12] and improved by Maslov and Fedoriuk [13] and Gutzwiller [14]. The approximation provides a full scattering amplitude with the possibility of all sorts of interferences. Moreover, no explicit assumptions about the two-electron continuum wave function are necessary. For collisions near threshold we make two additional ap-

proximations in the present calculation. They can be justified within the classical dynamics from which the semiclassical S matrix will be constructed. First, we calculate only the partial wave for total angular momentum L=0. By scaling the phase space variables (p_i,q_i) of the classical Hamiltonian with the energy E it can be shown that all partial waves contribute like the S wave in the limit $E \to 0$ [15]. Second, we restrict the calculation to an interelectronic angle of 180° which is a fixed point in the classical equations of motion. This means physically that the orbit of the bound electron becomes polarized during the approach of the projectile electron, with the geometry of $\Theta=180^{\circ}$ being energetically favored (minimum repulsion between the electrons). Furthermore, it is known from studies below [16] and above [7,8] threshold that the "bending" motion in Θ can be separated to a good approximation. In this context the close agreement of results from classical dynamics with and without the above approximations is also remarkable [17]. Most convincingly, however, the approximations are justified a posteriori by the excellent agreement with the experiment to be demonstrated below.

The simplified problem has 2 degrees of freedom, the radial distances between the electrons and the nucleus. In atomic units it is described by the Hamiltonian

$$H = \frac{p_1^2}{2} + \frac{p_2^2}{2} - \frac{1}{r_1} - \frac{1}{r_2} + \frac{1}{r_1 + r_2}.$$
 (1)

In the "one-dimensional" world, a cross section takes the form of a probability, directly related to the S matrix. The initial bound state appears as a classical Kepler orbit with energy ϵ' . The semiclassical scattering amplitude for ionization can be cast into the form

$$S_{\epsilon,\epsilon'}(E) = R(\epsilon', E)^{-\frac{1}{2}} \sum_{\text{cl.traj.}} \left| \frac{\partial r'}{\partial \epsilon} \right|_{\epsilon'}^{\frac{1}{2}} \exp\left\{ \frac{i\Phi}{\hbar} - \frac{i\nu\pi}{2} \right\},$$
(2)

where $R(\epsilon', E)$ is the normalization which ensures the unitarity of S. The classical probability for an individual trajectory is measured by $R(\epsilon', E)^{-1} \partial r' / \partial \epsilon$. Each trajectory accumulates a phase, which is defined by the classi-

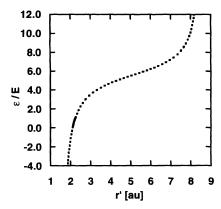


FIG. 1. Energy dependence ϵ of the projectile on its initial position 200 a.u.+r' for a total energy of 0.1 a.u. The inverse derivative of this function enters Eq. (2); see text. The different events, exchange (dotted, negative ϵ), ionization (solid), and excitation (dotted, positive ϵ), are indicated.

cal action $\Phi(\epsilon, \epsilon', E) = \int q_1 dp_1 + \int q_2 dp_2$ and a contribution of $\nu\pi/2$ from caustics along the trajectory [14]. The form of the semiclassical scattering amplitude in Eq. (2) is similar to Miller's "classical S matrix" [18] from which it can be derived. Since we use an unusual form of the prefactor, we sketch an alternative direct derivation of Eq. (2). The "canonical" prefactor in the semiclassical propagator contains $|\det A|$ with the 2 × 2 Jacobi matrix $A = \partial x'/\partial p$ between the final momenta $p(t \to \infty)$ and the initial positions $\mathbf{x}' = \mathbf{x}(t \to -\infty)$. Energy conservation of the S matrix reduces \mathbf{x}' to a one parameter manifold, and consequently the matrix \mathcal{A} to a simple derivative which can be represented in any suitable set of variables. We find the position of the initial free electron r' and its energy ϵ after the collision most convenient to describe ionization. The normalization R depends upon the variables used for A and is analytically known.

An overview over all events, excitation, (classical) exchange, and ionization, can be obtained by scanning the initial conditions $r'_0 + r'$ over one period of the bound electron with fixed energy ϵ' (Fig. 1). The distance r'_0 is arbitrary, but large enough so that the result is independent of r'_0 . Reading the plot from the right side it can be interpreted as a continuous energy transfer from the projectile electron, whose energy is shown, to the target electron. For $\epsilon > 0$ the dotted line marks the excitation regime. At some r' the projectile transfers enough energy to ionize the H atom (solid line). Losing even more energy at smaller r' the projectile eventually becomes bound in exchange for the target electron (dotted line, $\epsilon < 0$). The interval of initial conditions gives the normalization $R = \Delta r'$.

To determine the scattering amplitude we have to sum over all trajectories which contribute to Eq. (2). They are given as intersections of $\epsilon(r')/E$ in Fig. 1 with a horizontal line at energy ϵ/E . Since $\epsilon(r')/E$ is monotonic only one intersection exists so that a *single* trajectory

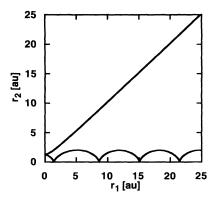


FIG. 2. Ionizing trajectory for initial bound state H(1s) at E=100 meV, leading to a final energy for one electron of $\epsilon=68.2$ meV.

fulfills a set of boundary conditions ϵ, ϵ' . The (analytic) proof of this remarkable fact will be given elsewhere [15]. A typical ionizing trajectory is shown in Fig. 2.

Moreover, the action is symmetric under electron exchange in the final channel, $\Phi(\epsilon, \epsilon', E) = \Phi(E - \epsilon, \epsilon', E)$. Consequently, Eq. (2) collapses to

$$S_{\epsilon,\epsilon'}(E) = R(\epsilon', E)^{-\frac{1}{2}} \left| \frac{\partial r'}{\partial \epsilon} \right|_{\epsilon'}^{\frac{1}{2}}, \tag{3}$$

where the phase has already been omitted, since it is irrelevant for the the symmetrized, differential ionization probability

$$P_{\epsilon}(E) = \left[S_{\epsilon,\epsilon'}(E) + S_{E-\epsilon,\epsilon'}(E) \right]^2. \tag{4}$$

The total ionization probability P(E), defined by the integral $\int_0^E P_{\epsilon}(E)d\epsilon$, is in excellent agreement with all data points of the threshold experiment [2] up to excess energies as high as 10 eV (Fig. 3). Written in the form $P(E) \propto E^{\alpha(E)}$ the exponent is $\alpha = 1.1268$ in the limit

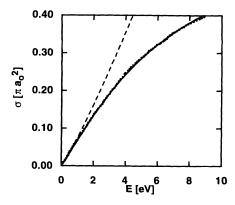


FIG. 3. The total ionization cross section for electron impact on H(1s). The experimental data points are taken from Ref. [2]. The calculated cross section (solid) has been normalized to the experimental data at 5.84 eV. The dashed line is the Wannier cross section $\sigma(E) = \sigma_0 E^{1.1268}$.

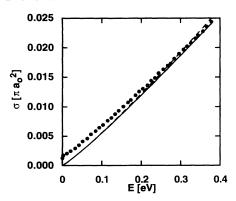


FIG. 4. Detail of Fig. 3 close to the threshold E=0. Note that the theoretical curves have not been corrected for the experimental energy resolution of $\Delta E=0.06$ eV.

 $E \to 0$ as calculated by Wannier (see Fig. 4). However, as can be seen from Fig. 4, the Wannier cross section and the (semi)classical cross section differ for finite E quantitatively. As pointed out by McGowan and Clarke the cross section does not follow any constant power law E^{α} beyond roughly 3 eV. The reason can be found in the differential ionization probability $P_{\epsilon}(E)$ according to Eq. (4). It is shown in Fig. 5 for different energies. Close to threshold, the electrons share the energy most likely equally [maximum at $\epsilon/E = 1/2$, Fig. 5(a)]. The shape of the energy distribution agrees qualitatively with classical calculations [7]. However, it does not confirm predictions of a flat energy distribution from earlier WKB formulations [4]. Roughly between 3 eV and 8 eV excess energy, the maximum of the electron distribution changes from equal sharing of energy to a preferred fast (projectile) electron ($\epsilon/E \approx 0$). The core of the transition regime [Fig. 5(b)] is characterized by small deviations (less than 1%) from a flat distribution. The extremely uneven energy sharing beyond the transition region [Fig. 5(c)] is familiar from energetic collisions: a fast projectile electron loses only energy of the order of the target binding energy.

The structural change in the form of the differential cross section, from a maximum to a minimum for equal energy sharing at a critical energy $E_{\rm crit}=3.3~{\rm eV}$ (open square in Fig. 6), defines naturally the energy range of qualitative threshold behavior. Threshold behavior in the total cross section is characterized by the possibility of a fit with a power law.

The present work is not an exact quantum calculation. Moreover, it has been restricted to the collinear configuration. Yet, for the first time it has been possible to reproduce the form of the experimental cross section accurately for all energies (0–10 eV) covered in the threshold experiment by McGowan and Clarke [2]. A structural change in the differential cross section at a critical excess energy provides a natural limit for the threshold range and explains why the total cross section does not follow any power law beyond this energy. Perhaps most remarkable is the fact that only a single trajectory contributes to the collinear semiclassical S matrix. Apart from the symmetrization for identical particles imposed by the Pauli principle, the result is in fact classical.

Overall, the semiclassical version of Feynman's path integral offers a transparent framework for the formulation of the ionization process particularly but not exclusively close to threshold. Numerical details of the calculation, concerning the Coulomb singularities and the necessity to integrate out to extremely large distances (10^8 a.u.) in order to compute small energy sharings $\epsilon/E \ll 1$ reliably, can be tedious. Nevertheless, without the collinear restriction and L=0, the approach described here can be used in the future to determine the absolute total cross section, various angular distributions, and the spin asymmetry, an important observable close to threshold [10]. Semiclassical S matrix theory is in particular very promising for Coulomb problems, since it naturally incorporates the effect of long range forces without explicitly

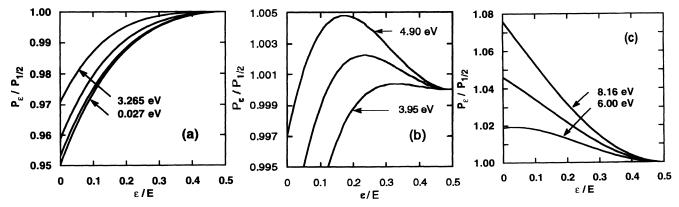


FIG. 5. Differential ionization probability $P_{\epsilon}(E)$ according to Eq. (4), normalized to its value for $\epsilon/E = 1/2$: (a) For energies close to threshold, represented as squares in Fig. 6; (b) for energies in the transition region, represented by circles in Fig. 6; (c) for energies beyond the transition region, marked as triangles in Fig. 6.

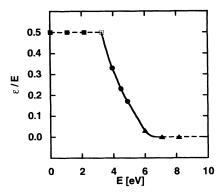


FIG. 6. Maximum of the differential ionization probability [Eq. (4)] as a function of total energy E. The dashed lines mark constant maxima at the positions $\epsilon/E = 1/2$ for small energy and $\epsilon/E \approx 0$ for higher energies. The data points indicate the energies E of the curves $P_{\epsilon,\epsilon'}(E)$ plotted in Fig. 5.

specifying boundary conditions.

Discrepancies between a full quantum calculation or very precise measurements (if they become available in the future) and the semiclassical scattering results would raise interesting fundamental questions concerning the commutation of the limits $\hbar \to 0, E \to 0$, and $t \to \infty$. These limits are literally tested in a threshold process, when in the limit of $E \to 0$ the electrons take a time $t \to \infty$ to escape. Furthermore, the measurement process plays an important role near the threshold, since the correlation of the electrons for extremely long times and distances, as assumed theoretically, probably does not hold experimentally.

I would like to thank F. Grossmann, Rick Heller, M. Lubell, M. Sepulveda, A. Temkin, S. Tomsovic, and D. Wintgen for many helpful discussions. I also gratefully acknowledge support from the Humboldt Foundation in

the form of a Feodor-Lynen fellowship.

- [1] G. H. Wannier, Phys. Rev. 90, 817 (1953).
- [2] J. W. McGowan and E. M. Clarke, Phys. Rev. 167, 43 (1968).
- [3] P. Marchand, C. Paquet, and P. Marmet, Phys. Rev. 180, 123 (1969); S. Cvejanović and F. H. Read, J. Phys. B 7, (1974).
- [4] A. R. P. Rau, Phys. Rev. A 4, 207 (1971).
- [5] R. K. Peterkop, J. Phys. B 4, 513 (1971); J. M. Feagin,
 J. Phys. B 17, 2433 (1984); D. S. Crothers, J. Phys. B
 19, 463 (1986).
- [6] A. Temkin, Phys. Rev. Lett. 49, 365 (1982).
- [7] F. H. Read, J. Phys. B 17, 3965 (1984); M. Gailitis, J. Phys. B 19, L697 (1986).
- [8] A. K. Kazansky and V. N. Ostrovsky, Phys. Rev. A 48, R871 (1993).
- [9] J. B. Donahue et al., Phys. Rev. Lett. 48, 1582 (1988).
- [10] X. Q. Guo et al., Phys. Rev. Lett. 65, 1857 (1990); M.
 S. Lubell, Phys. Rev. A 47, R2450 (1993).
- [11] I. Bray and A. T. Stelbovics, Phys. Rev. Lett. 70, 746 (1993).
- [12] J. M. van Vleck, Proc. Acad. Natl. Sci. U.S.A. 14, 178 (1928).
- [13] V. P. Maslov and M. V. Fedoriuk, Semi-Classical Approximations in Quantum Mechanics (Reidel, Boston, 1981).
- [14] M. C. Gutzwiller, Chaos in Classical and Quantum Mechanics (Springer, New York, 1990).
- [15] J. M. Rost (to be published).
- [16] J. M. Rost and J. S. Briggs, J. Phys. B 24, 4293 (1991);
 H. R. Sadeghpour and C. H. Greene, Phys. Rev. Lett.
 65, 313 (1990); G. S. Ezra, K. Richter, G. Tanner, and
 D. Wintgen, J. Phys. B 24, L413 (1991); J. Müller, J.
 Burgdörfer, and D. Noid, Phys. Rev. A 45, 1471 (1992).
- [17] L. G. J. Boesten, H. G. M. Heideman, T. F. M. Bonsen, and D. Banks, J. Phys. B 9, L1 (1976); L. G. J. Boesten, D. Banks, and H. G. M. Heideman, J. Phys. B 9, L97 (1976).
- [18] W. H. Miller, Adv. Chem. Phys. 25, 69 (1974).